Title	Mechanical behavior of ProTaper Universal F2 finishing file under various curvature conditions: A finite element analysis study
Author(s)	Gao, Y; Cheung, GSP; Shen, Y; Zhou, X
Citation	Journal of Endodontics, 2011, v. 37 n. 10, p. 1446-1450
Issued Date	2011
URL	http://hdl.handle.net/10722/143359
Rights	NOTICE: this is the author's version of a work that was accepted for publication in Journal of Endodontics. Changes resulting from the publishing process, such as peer review, editing, corrections, structural formatting, and other quality control mechanisms may not be reflected in this document. Changes may have been made to this work since it was submitted for publication. A definitive version was subsequently published in Journal of Endodontics, 2011, v. 37 n. 10, p. 1446-1450. DOI: 10.1016/j.joen.2011.06.003

Mechanical behavior of ProTaper Universal F2 finishing file under various curvature conditions: A finite element analysis study.

Yuan Gao[1], DDS, PhD, Gary S.P. Cheung[2], MSc, MDS, PhD,
Ya Shen[3], DDS, PhD, Xuedong Zhou[1], DDS, PhD

1 State Key Laboratory of Oral Diseases, West China College & Hospital of Stomatology, Sichuan University, Chengdu, China
2 Area of Endodontics, Comprehensive Dental Care, Faculty of Dentistry, University of Hong Kong, Hong Kong
3 Division of Endodontics, Department of Oral Biological & Medical Sciences, Faculty of Dentistry, University of British Columbia, Vancouver, Canada

Corresponding author: Prof. Xuedong Zhou
Professor and Dean
State Key Laboratory of Oral Diseases
West China College & Hospital of Stomatology
Sichuan University
14, 3rd section of RenMin Nan Road, Chengdu, China, 610041.
E-mail: zhouxd@scu.edu.cn
Tel: +86-28-85501439 Fax: +86-28-85582167

Acknowledgments

This study was supported by Open Research Fund Program of the State Key Laboratory of Oral Diseases of China (Grant No. SKLOD008) and Youth Fund Program of Sichuan University (Grant No. 2008072).The authors deny any conflicts of interest related to this study.

Mechanical behavior of ProTaper Universal F2 finishing file under various curvature conditions: A finite element analysis study.

Intrudution: To visualize the stresses and strain distribution patterns in ProTaper Universal F2 files and to establish the stress- and strain-curvature relationship for this instrument under various conditions by using a dynamic, 3-dimensional finite-element model. **Methods:** An accurate geometrical model of a ProTaper Universal F2 instrument was created. Two short, straight tubes were also modeled to represent the parts of root canal apical and coronal to the curvature. Then, the file was constrained to a curve of varying degree, curve length and position. The maximum Von Mises stress and strain on the tension side of the instrument was measured at 5-degree intervals in a numerical simulation package (LS-DYNA, Livermore software). **Results:** The mechanical performance of the ProTaper F2 file under various conditions was simulated. A long curvature length produced lower values of stress and strain under the same angle of curvature. Increase in the curvature angle generally induces higher stress and strain. For the same degree and curve length, the stress and strain increased if the curved portion was situated further up the shaft of the instrument i.e. with larger diameter. **Conclusions:** The dynamic, numerical model may be used to evaluate and compare the effect of various root canal curvatures on the behavior of different designs of root canal instrument. The magnitude of stress and strain imposed on the instrument is influenced by the abruptness and degree of curvature, as well as the location of the curved portion.

Key Words: Curvature; finite element analysis; ProTaper Universal; bending stress; nickel titanium; rotary instrument

Introduction

A thorough understanding of the configuration of curved root canal system is of great importance for successful root canal preparation (1). As is commonly known, substantial curvature is an obstacle to root canal instrumentation. With an increase in canal curvature, the stress on the instrument becomes greater and the risk of breakage increases. Flexural fatigue also develops if the instrument is to rotate inside a curved root canal. This is especially true for nickel-titanium (NiTi) rotary instruments (2). In this regards, the stresses and strains experienced by the instrument are of great clinical significance, as they are intimately related to the chance of instrument separation in use (3-5).

There are many techniques to evaluate the root canal curvature. The most common and simplest method is that published by Schneider (6), which provides a description of the angle. Pruett et al. (7) indicated that it is not possible to define a curvature based on the angle alone, because canals can have the same angle while having different radii of curvature. It has been pointed out that to define the canal curvature mathematically and unambiguously, the angle, radius and length of the curve should all be considered and described (8, 9). Recently, microcomputed tomography (micro-CT) and mathematical modeling has been used to analyze the root canal system 3-dimensionally (1, 10). However, such complex descriptive parameters of the curvature are difficult to communicate to the clinician or the patient. Nor would it be easy to control for purpose of comparing the efficacy of root canal instruments or instrumentation techniques in laboratory experiments.

Little is known about the development and distribution of stresses and strains, an important factor related to instrument fracture and fatigue, of a rotary file that is subjected to bending in a curved root canal. Stress concentration sites are the most likely locations for fracture and fatigue-crack initiation and, hence, knowledge of the distribution of stresses in an instrument can help reduce the chance of fracture during clinical use (11). Finite element analysis (FEA) has been increasingly used to study the mechanical behavior of endodontic files under bending or torsion (11-16). While some had used the Schneider's description for the curvature in their study (14), with a concentrated load at one point and leaving the file to curve naturally in the form of cantilever bending, others took into account the effect of the radius of curvature (15). The location of the (beginning and finishing point of the) curvature

in relation to the length of the instrument is an important concern – as it is well-known that rotary files seem especially vulnerable in canals with a mid-root versus apical curve – but this has never been reported.

The main advantage of computational methods is the ability to evaluate aspects of the mechanical behavior of the instruments (e.g. stress and strain, and their distribution), which are difficult to measure through laboratory or in vivo tests. Moreover, different working conditions, by simply changing various boundary conditions, can be evaluated and compared readily in a numerical model. Given the potentials of FEA and the importance of canal curvature in endodontics, the purpose of this study was to examine the stresses and strain distribution patterns in NiTi (ad *modem* ProTaper Universal F2) files under different curvature conditions by using a dynamic, 3-dimensional FEA.

Materials and methods

Geometry and 3D mesh model

ProTaper Universal (finisher) F2 file (Dentsply Maillefer, Ballaigues, Switzerland) was used for the current study. A 3-dimensinal (3D) CAD model was created using a modeling software (CATIA; Dassault Systems, France) according to the information provided by the manufacturers, and from data in the literature (17). To obtain the value for the pitch of the file (Fig. 1A), the instrument was measured under an optical, travelling microscope. The 3D geometrical model was obtained for the cutting part, i.e. apical 16 mm of the file, which was then meshed with hexahedral and tetrahedral elements in software (Gambit; Fluent, Lebanon, NH). The meshed model consisted of 29362 elements (Fig. 1B).

Constitutive model and numerical simulation

The mechanical behavior of nickel-titanium alloy is highly non-linear (18). Briefly, the stress-strain behavior of NiTi comprises a linear elastic deformation of the parent phase (austenite), a pseudoelastic plateau during which stress-induced phase transformation from austenite to martensite occurs, followed by elastic and then plastic deformation of the martensitic phase. Together with the unloading curve, a hysteresis loop is formed (18). The Young's modulus of the martensite is different from that of the austenite. In addition, there

is a slight difference between the material's response in tension and compression (19). This non-linear mechanical behavior during the stress-induced martensitic transformation, both forward (austenite to martensite) and reverse transformation, are the key to explain the superelastic property of this material. For this study, the parameters used were as follow: Austenite Young's modulus = 50,000 MPa; Martensite Young's modulus = 34,000 MPa; Poisson ratio (austenite or martensite) 0.3; Initial stress for austenite-to-martensite transformation = 500 MPa; Final austenite-to-martensite stress = 600 MPa; Initial stress for martensite-to- austenite (reverse) transformation = 300 MPa; Final martensite-to-austenite stress = 200 MPa; Recoverable strain or maximum residual strain = 0.07; a material constant (Alpha) that measures the difference in the material's response between tension and compression: $\alpha = 0.12$. The 3D meshed model and the above values were entered into a numerical simulation software (LS-DYNA; Livermore Software Technology, Livermore, California, USA).

For the dynamic bending analysis, a pair (3D model) of straight tubes were created by the Gambit software (Fluent), to represent those parts of a canal that constrains the file coronal and apical to the curvature. That is, the curved part of the instrument was positioned between a straight coronal and a straight apical portion (Fig. 1 C, D). This would allow the simulation of mid-root curvatures or curve that begins at any part of the canal, by adjusting the location of the two tubes, instead of merely testing the cantilever bending characteristic of the instrument. Combinations of different lengths for the curved portion and for the straight apical (tube) portion were created, including: a 1 mm-long apical portion (inside the tube) with a curved portion of 2 to 5 mm in length; a 2 mm-long apical portion with a 2 to 4 mm-long curve; a 3 mm apical portion with a 2 or 3 mm curve; a 4 mm apical portion with a 2 mm curved portion (Fig. 2 and 3). That is, various combinations of the location and abruptness of the curvature for the apical 6 millimeters of the instrument was reproduced. The (arc portion of the) file was forced to bend by adjusting the distance and angulation of the two tubes with respect to each other, to simulate the various degrees of curvature experienced in a root canal. The curvature was described, using a method similar to that of Weine (20) and Pruett et al. (3), as the angle between the two axes for the coronal and the apical portion of the instrument (i.e. of the two tubes) (Fig. 1D). The maximum

Von Mises stress and strain on the tension side (Fig. 1E) of the instrument was measured at 5-degree intervals from 0 to 90 degrees. Stress values exceeding 1400 MPa, being the ultimate tensile strength of NiTi (18), were deemed to result in breakage or failure of the instrument. Numerical simulations were performed in the LS-DYNA (Livermore Software Technology) software package. The LS-PrePost module (Livermore Software Technology) was used for calculating the curvature, the Von Mises stress and strain to produce the graphical results.

Results

At various curvature conditions and locations, the maximum stress and strain at the nodes on tension side were plotted for the instrument (Fig. 4). The relationship was nonlinear, and appeared to correspond to the transformation between phases of the NiTi material on the stress-curvature plot. At the transformation or the "plateau" region of the plot, the degree of curvature continued to increase but with only a small rise in stress (Fig. 4A). The strain-curvature plot showed the amount of distortion as a function of the curvature (Fig. 4B). The general sequence of the curves (i.e. order of the lines from left to right) mirrored closely that of the stress-curvature plot.

When the arc length for the curved portion was concerned, the longer the curve length portion, the lower the stress developed in the instrument (Fig. 2). There was a sharp rise in the maximum Von Mises stress for instrument with a 2 mm-long curved part; the rise was even sharper when the curve was situated further up the shaft of the instrument (Fig. 4A). In general, shifting the curved portion of the instrument from apical to a more coronal position resulted in an increase in the stress and strain values under the same arc length and angle of curvature (Fig. 4). For different angles of curvature the distribution of Von Mises stress and strain changed (Fig. 3). With an increasing angle, the stress value rose rapidly at first, then experienced a plateau stage and rose further (Fig. 4A); the angle of curvature did not seem to influence substantially the stress level at the plateau region. Angles beyond 45 degrees generally incurred high strain values, beyond the stress-induced martensitic transformation of the material (Fig. 4B).

Discussion

In the last decade, NiTi rotary instruments were introduced to facilitate instrumentation of curved canals. They were shown to possess good shaping ability (21, 22) and result in an improved success rate of treatment (23). There is a concern for unexpected instrument separation in use (2, 7, 21), with a potential effect on the healing outcome of treatment depending on when this occurs in relation to the stage of root canal preparation (24).

In this present study, we incorporated three parameters pertaining to the characters of curved root canals: the length of the curve (i.e. gentle vs abrupt curve), the angle and the position of the curved portion. Not measured in this study, the radius of the curvature is well-known for its impact on the fatigue life of rotary instruments (3-5). While the curved portion of the file resembled an arc whose radius may be estimated by best-fitting a circle on it (25), it was commented that the trajectory assumed by the instrument is not exact on a circle but is a plain curve of a higher-order equation (26). This is true considering that the rotary instrument is a tapered, not a prismatic beam. In this study, the curve length was used, instead, to represent the severity and abruptness of curvature; the FEA model would simulate the non-circular trajectory of the instrument due to the bending moment. Although we did not specify the radius of curvature in this study, a lengthy curved-portion always means a large radius obviously. That is, the shorter the length of curvature, the more abrupt the deviation at same the degree of curvature, hence representing a smaller radius of curvature. Our observation of the "curve-accommodating capacity" of the rotary file is in agreement with the results of laboratory experiments (7，27-29) suggesting that the radius of curvature (an estimation only, as the actual trajectory is not part of circle) was the predominant factor for fatigue life of the instrument.

From the stress and strain result of the group with 2mm curve (arc) length, there was a sharp rise in the maximum Von Mises strain for instrument with increasing curvature angle. The rise was sharper than any other groups of a longer arc length (Fig.2). Explanation of the effect of arc length is complex, but can be grossly simplified by stating that stress and strain on the instrument is inversely related to the radius of curvature (12, 14). Therefore, as the curve (arc) length decreases, the reduced radius of curvature will lead to an increase in stress and strain for the instrument (Fig.2). The fatigue life is negatively affected, which has been

shown in many other studies (7, 12). The results here indicated that the effect of the length (and hence radius) of curvature as an independent variable which should be considered when evaluating root canal instrumentation.

When the curved portion of the instrument was shifted from an apical to a more coronal position, the rise in stress and strain was even sharper at the same arc length and angle of curvature. Instruments of a large diameter will have lower fatigue lives, compared with smaller instruments (2, 7). Therefore, considering cyclic fatigue as a contributor to instrument failure, if the curvature is situated closer to a coronal position, the rotary file will be in a more vulnerable position. But then, the radius of curvature (as indicated by the curve length in this study; Fig. 2) remains the most important factor in governing the fatigue failure, a fact that is well know to most clinicians nowadays.

Nickel-titanium instruments rotating with a curvature are subjected to tensile and compressive stresses with the concave side of the instrument under compression and the outer surface under tension (2). Any stress concentrations sites are likely to be the locations for fracture or fatigue-crack initiation. Thus, avoiding such stress concentrations in the rotary files should improve their fracture resistance during clinical use. Since most root canal curvatures are situated close to the apex (8), we simulated such curve for the apical 6 mm of the instrument only. Numerically, it is perfectly possible to map all combinations of the length, location and angle of curvature for the entire length of the instrument systematically. The results here showed that decreasing the curve length and increasing the curvature angle bring about a rise in the stress and strain levels. And the plot corresponded well with the stress-induced martensitic transformation of superelastic NiTi material from which the instruments are made.

It is widely accepted that instruments of a smaller diameter are able to withstand a higher number of cycles of flexural fatigue loading (rotational bending) than those larger instruments of the same design (2, 3, 7, 21, 29). Our finding clearly demonstrated that positioning the simulated curvature away from the tip of instrument, i.e. bending that wound affect a cross section with a larger diameter due to the taper, would result in increasing levels of stress and strain.

FEA is recognized to have an important role in visualizing the behavior and evaluating the design of biomedical components. Our work focused on the study of the stress and strain distribution of a NiTi rotary instrument under different curvature conditions that may be encountered clinically. Curvatures of various degrees and radii situated both at the apical and (close to) the mid-root regions were simulated in the present study. Traditionally, torsion or fatigue tests were performed separately in the laboratory, with the latter typically done in simulated canals with a fixed curvature. It could be difficult to extrapolate to the clinical situation for all types of root canals, as their curvature may assume a different angle, radius or curve length. As the geometry of the root canal can hardly be reduced to a single parameter or a standard condition (for laboratory experimentation), finite element analysis is able to provide a comprehensive and quantitative characterization for the instrument operating in there. Complete set of data under various curvature conditions may be obtained and form the basis of a usable database that could help clinicians choose the most appropriate (design of) instrument for a particular type of canal curvature.

A limitation of the present study is related to the hypothesis of the test model that the file was operating with minimal friction. In actual situation, the stresses may differ when the instrument is actively filing the dentin wall during clinical use. Attempt is in place to simulate the simultaneous application of torsion and bending moments on the rotary instrument.

In summary, a method of simulation the various curvature conditions of the root canal is proposed. A dynamic numerical model was used to examine the behavior of rotary instruments (of linear or nonlinear mechanical properties including superelastic behavior) in these different curvature conditions for the development and distribution of stress and strain. The stress and strain of a rotary file is affected by the arc length (abruptness of curve), degree of curvature and the location of the curved portion along the instrument.

References

1. Lee JK, Ha BH, Choi JH, Heo SM, Perinpanayagam H. Quantitative three-dimensional analysis of root canal curvature in maxillary first molars using micro-computed

tomography. J Endod 2006;32:941-5.

2. Cheung GS. Instrument fracture: mechanisms, removal of fragments, and clinical outcomes. Endod Top 2009;16:1-26.
3. Turpin YL, Chagneau F, Vulcain JM. Impact of two theoretical cross-sections on torsional and bending stresses of nickel-titanium root canal instrument models. J Endod 2000;26:414-7.
4. Berutti E, Chiandussi G, Gaviglio I, Ibba A. Comparative analysis of torsional and bending stresses in two mathematical models of nickel-titanium rotary instruments: ProTaper versus ProFile. J Endod 2003;29:15-9.
5. Xu X, Eng M, Zheng Y, Eng D. Comparative study of torsional and bending properties for six models of nickel-titanium root canal instruments with different cross-sections. J Endod 2006;32:372-5.
6. Schneider SW. A comparison of canal preparations in straight and curved root canals. Oral Surg Oral Med Oral Pathol 1971;32:271–5.
7. Pruett JP, Clement DJ, Carnes DL, Jr. Cyclic fatigue testing of nickel-titanium endodontic instruments. J Endod 1997;23:77-85.
8. Schafer E, Diez C, Hoppe W, Tepel J. Roentgenographic investigation of frequency and degree of canal curvatures in human permanent teeth. J Endod 2002;28:211-6.
9. Zhang R, Hu T. Root canal curvature. (letter to editor and discussions) Int Endod J 2010;43:616-21.
10. Peters OA, Laib A, Ruegsegger P, Barbakow F. Three-dimensional analysis of root canal geometry by high-resolution computed tomography. J Dent Res 2000;79:1405-9.
11. Kim HC, Kim HJ, Lee CJ, Kim BM, Park JK, Versluis A. Mechanical response of nickel-titanium instruments with different cross-sectional designs during shaping of simulated curved canals. Int Endod J 2009;42:593-602.
12. Necchi S, Taschieri S, Petrini L, Migliavacca F. Mechanical behavior of nickel-titanium rotary endodontic instruments in simulated clinical conditions: a computational study. Int Endod J 2008;41:939-49.
13. Kim TO, Cheung GS, Lee JM, Kim BM, Hur B, Kim HC. Stress distribution of three NiTi rotary files under bending and torsional conditions using a mathematic analysis. Int

Endod J 2009;42:14-21.

14. Zhang EW, Cheung GS, Zheng YF. Influence of cross-sectional design and dimension on mechanical behavior of nickel-titanium instruments under torsion and bending: a numerical analysis. J Endod;36:1394-8.
15. He R, Ni J. Design improvement and failure reduction of endodontic files through finite element analysis: application to V-Taper file designs. J Endod 2010;36:1552-7.
16. Zhang EW, Cheng GS, Zheng YF. A mathematical model for describing the mechanical behavior of root canal instruments. Int Endod J 2011;44:72-6.
17. Camara AS, de Castro Martins R, Viana AC, de Toledo Leonardo R, Buono VT, de Azevedo Bahia MG. Flexibility and torsional strength of ProTaper and ProTaper Universal rotary instruments assessed by mechanical tests. J Endod 2009;35:113-6.
18. Hodgson DE, Wu MH, Biermann RJ (1990) Shape memory alloys. In: Davis JR, Allen P, Lampman SR, Zorc TB, Henry SD, Daguila JL, *et al* (eds). *Metals Handbook, vol. 2: Properties and Selection: Nonferrous Alloys and Special-Purpose Materials*, 10th edn. Materials Park, OH: ASM International, 1990. pp.897–902.
19. Rejzner J, Lexcellent C, Raniecki B. Pseudoelastic behavior of shape memory alloy beams under pure bending: experiments and modelling. Int J Mech Sci 2002;44: 665-86.
20. Weine FS. Endodontic Therapy. 3rd ed. St Louis, MO: CV Mosby; 1982. pp.256–340.
21. Bergmans L, Van Cleynenbreugel J, Wevers M, Lambrechts P. Mechanical root canal preparation with NiTi rotary instruments: rationale, performance and safety—status report for the American Journal of Dentistry. Am J Dent 2001;14:324-33.
22. Peters OA. Rotary Instrumentation: An Endodontic Perspective. Endodontics: Colleagues for Excellence. American Association of Endodontists: 2008 (Winter issue), pp. 2-7.
23. Cheung GS, Liu CS. A retrospective study of endodontic treatment outcome between nickel-titanium rotary and stainless steel hand filing techniques. J Endod 2009;35:938-43.
24. Spili P, Parashos P, Messer HH. The impact of instrument fracture on outcome of endodontic treatment. J Endod 2005;31:845-50.

25. Cheung GS, Darvell BW. Fatigue testing of a NiTi rotary instrument: part 1—Strain-life relationship. Int Endod J 2007;40:612–8.
26. Plotino G, Grande NM, Cordaro M, Testarelli L, Gambarini G. Measurement of the trajectory of different NiTi rotary instruments in an artificial canal specifically designed for cyclic fatigue tests. Oral Surg Oral Med Oral Pathol Oral Radiol Endod 2009;108:e152-156.
27. Zelada G, Varela P, Martin B, Bahillo JG, Magan F, Ahn S. The effect of rotational speed and the curvature of root canals on the breakage of rotary endodontic instruments. J Endod 2002;28:540-2.
28. Martin B, Zelada G, Varela P, Bahillo JG, Magan F, Ahn S, et al. Factors influencing the fracture of nickel-titanium rotary instruments. Int Endod J 2003;36:262-266.
29. Lopes HP, Moreira EJ, Elias CN, de Almeida RA, Neves MS. Cyclic fatigue of ProTaper instruments. J Endod 2007;33:55-57.

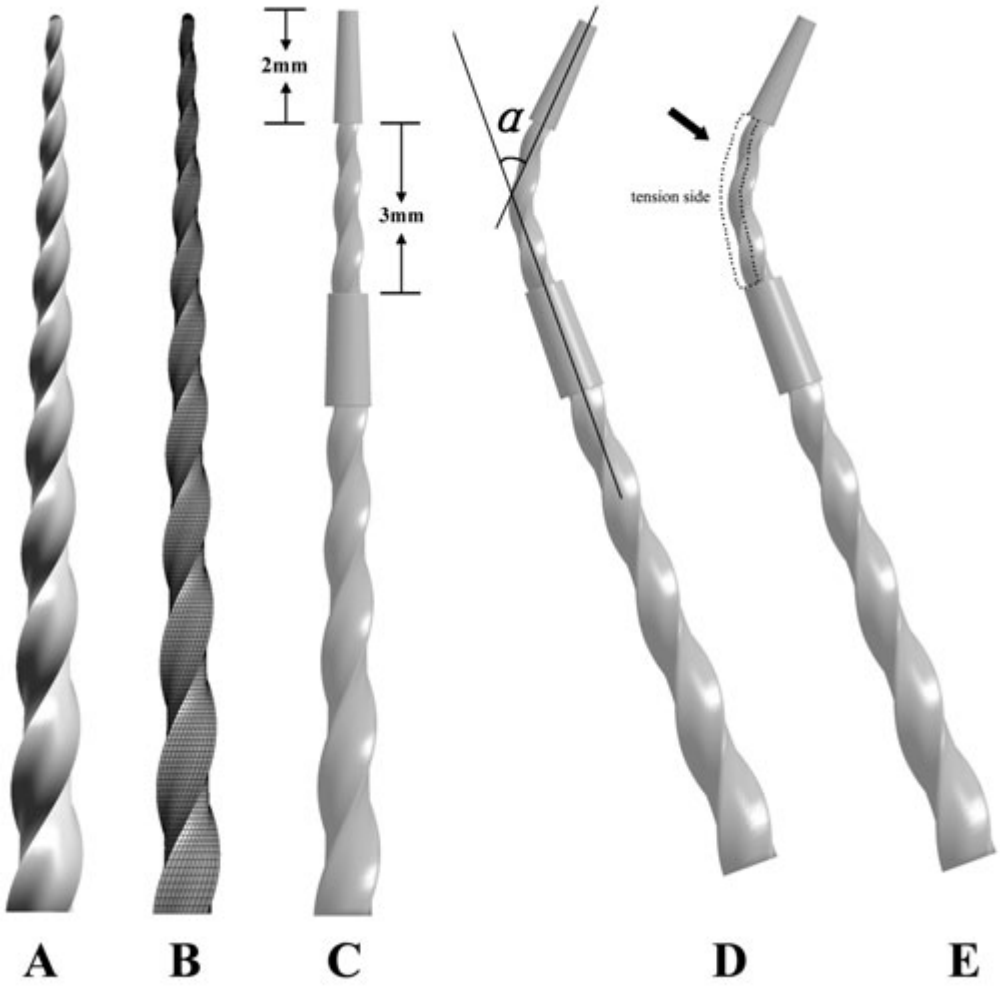

Figure 1 Computational model of the ProTaper F2 instrument: (A) CAD model based on the profile of a brand-new instrument; (B) The mesh model of F2 for finite element analysis; (C) The model of two 2mm-ong straight tubes fitted to the apical and coronal portion of the file, leaving a 3mm portion for bending; (D) Determination of the angle the curvature with the Weine's method; (E) The tension region of the curved instrument (dotted region).

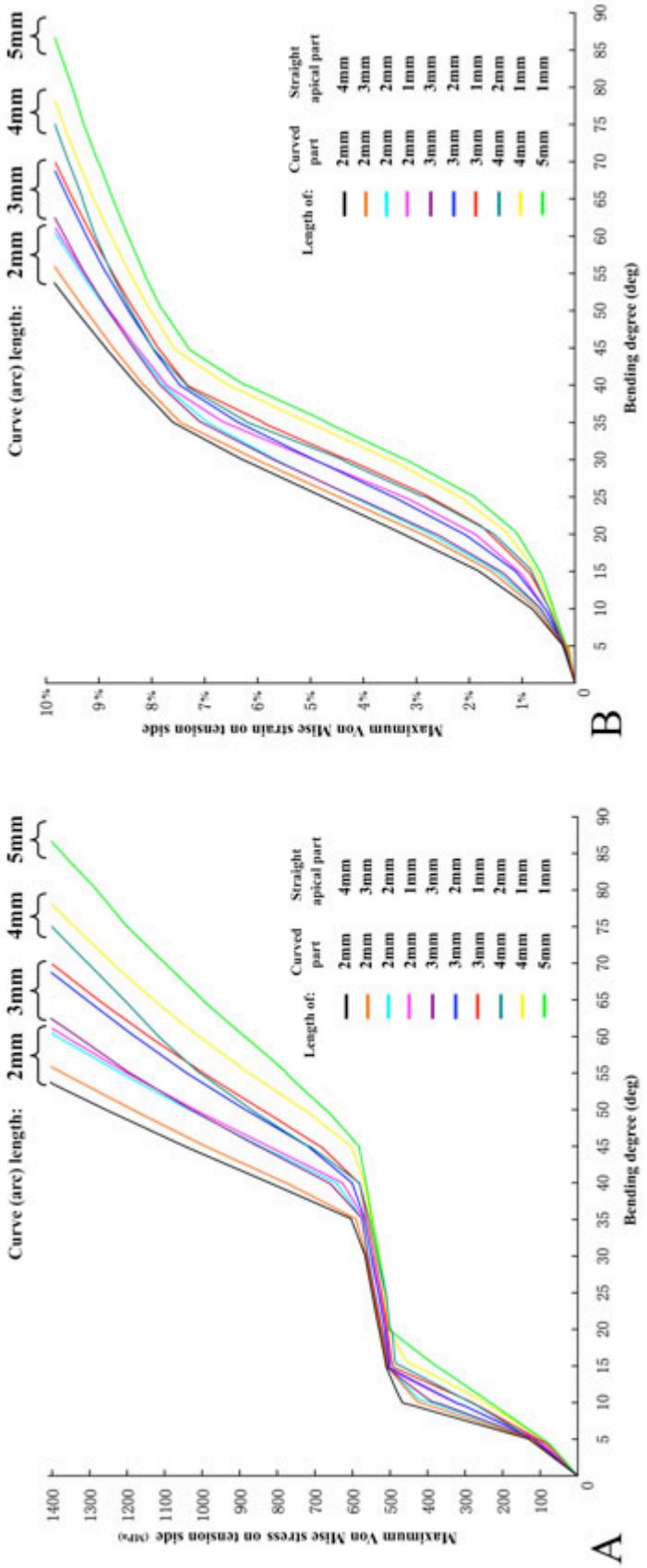

Figure 2. Maximum Von Mises stresses(A) and strains(B) developed in the F2 instrument under various curvature condition.

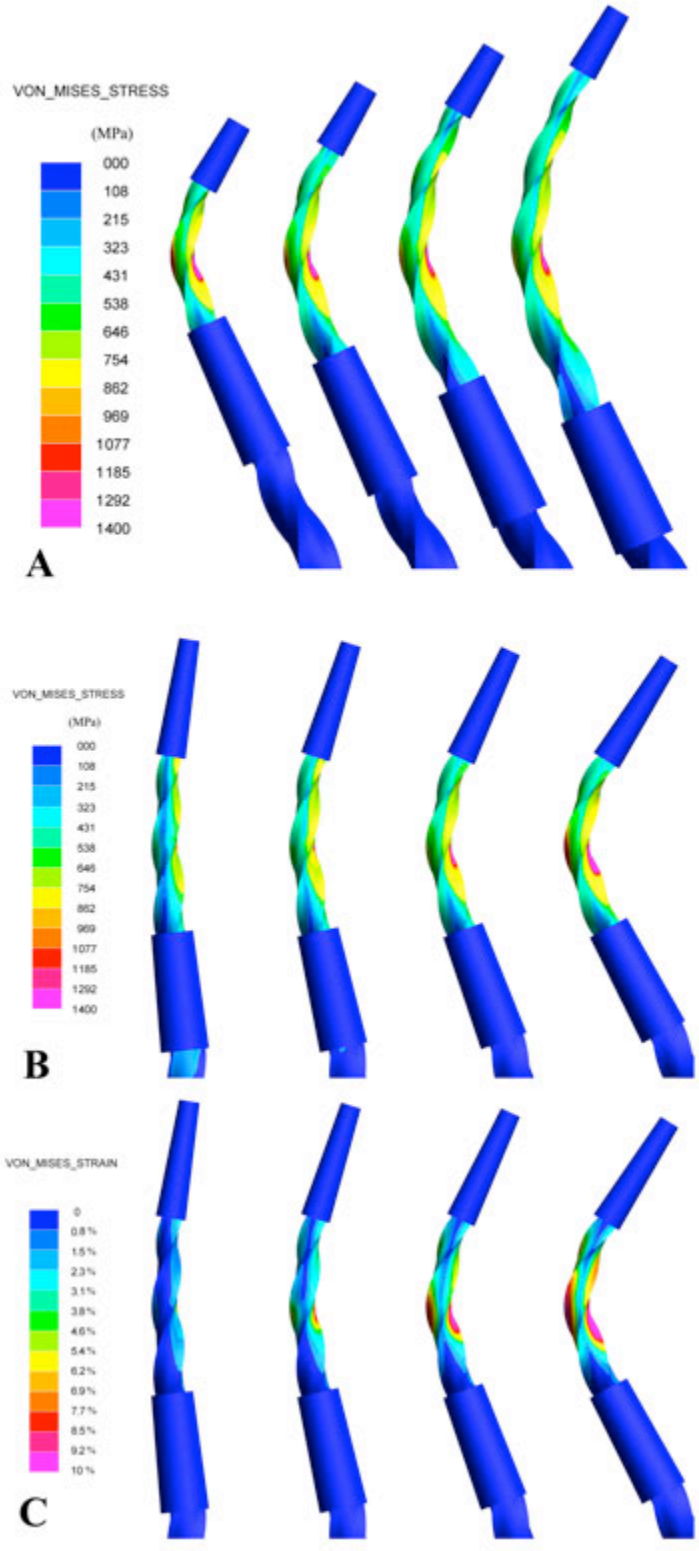

Fig 3. Contour map showing the distribution of Von Mises stresses and strains: (A) Von Mises stresses for the group with a 1mm straight apical part with different curved (arc) length ranging from 2 to 5mm at 55-degree curvature. (B&C) Von Mises stresses and strains for the group with a 2mm straight apical part and 3mm curved (arc) length at curvature angles of 15,30,45 and 60 degrees.